JACS
JOURNAL OF THE AMERICAN CHEMICAL SOCIETY
Communication
pubs.acs.org/JACS

Encapsulation of a Nerve Agent Detoxifying Enzyme by a Mesoporous Zirconium Metal–Organic Framework Engenders Thermal and Long-Term Stability

Peng Li,[†] Su-Young Moon,[†] Mark A. Guelta,[‡] Steven P. Harvey,[‡] Joseph T. Hupp,[†] and Omar K. Farha*[,†,§]

[†]Department of Chemistry and Chemical and Biological Engineering, Northwestern University, 2145 Sheridan Road, Evanston, Illinois 60208, United States

[‡]U.S. Army Edgewood Chemical Biological Center, 5183 Blackhawk Road, RDCB-DRC-C, Aberdeen Proving Ground, Maryland 21010-5424, United States

[§]Department of Chemistry, Faculty of Science, King Abdulaziz University, Jeddah 21589, Saudi Arabia

Supporting Information

ABSTRACT: Immobilized enzymes typically have greater thermal and operational stability than their soluble form. Here we report that for the first time, a nerve agent detoxifying enzyme, organophosphorus acid anhydrolase (OPAA), has been successfully encapsulated into a water-stable zirconium metal–organic framework (MOF). This MOF features a hierarchical mesoporous channel structure and exhibits a 12 wt % loading capacity of OPAA. The thermal and long-term stabilities of OPAA are both significantly enhanced after immobilization.

Nerve agents are the most toxic of all chemical weapons.[1,2] Development of antidotal therapy for chemical agent poisoning has been a significant research focus since World War II.[3,4] The use of catalytic enzymes for nerve agent detoxification has sparked widespread interest due to the excellent biocompatibility and high efficiency of these enzymes.[5−8] Organophosphorus acid anhydrolase (OPAA; EC.3.1.8.2) is a prolidase enzyme that catalyzes the hydrolysis of P−F, P−O, P−CN, and P−S bonds commonly found in toxic organophosphorus compounds and G-type chemical agents.[9] However, the use of OPAA in nerve agent detoxification applications is made difficult by the poor stability of this enzyme in organic solvents, at elevated temperature and when storing the enzyme long-term.[10] Field application requires that the enzyme antidote is easy to handle in dry powder form to reduce complicated storage logistics and the burden of shipping.[11]

Significant effort has been devoted to developing useful materials as solid supports for encapsulation of OPAA to afford stable and convenient formulation for use in chemical agent detoxification and detection. Previously, various materials including polymers,[12] silica gel,[13] functionalized mesoporous silicas (FMS),[14,15] and porous silica (PSi)[16] have been used to immobilize OPAA. For example, FMS encapsulated OPAA shows enhanced tolerance to organic solvents. Nevertheless, due to a lack of long-range ordering, the loading capacity of OPAA in FMS is usually very low (<0.01 wt %).[15] In addition, enhanced thermal and long-term stability of immobilized OPAA has not yet been achieved. Therefore, the development of new host materials is important for targeting both high enzyme loading and enhanced stability for OPAA immobilization.

Recently, metal–organic frameworks (MOFs),[17] a rapidly growing class of hybrid crystalline materials, have been shown to be effective for enzyme immobilization applications.[18] Several reports on the immobilization of enzymes into cage-like mesoporous MOFs (mesoMOFs) show higher loading of enzymes with superior stability compared to those incorporated into mesoporous silica.[19−21] However, the development of channel-type mesoMOFs for enzyme encapsulation has significantly lagged behind that of cage-like mesoMOFs. Nevertheless, it should be noted that the isoreticular synthesis strategy[22] has been used to produce channel-type MOFs with hexagonally arranged pores up to 10 nm in diameter.[23] Mesoporous zirconium-based MOFs are of interest for exploration in enzyme immobilization due to their excellent aqueous stability.[24,25] Ideally, an enzyme support should have a hierarchical pore structure with large pores for enzyme immobilization and smaller, enzyme-free pores for reactant delivery and product expulsion. Among these reported zirconium MOFs, frameworks with *csq*-net topology[26−29] featuring large hexagonal and small triangular channels could potentially serve as ideal enzyme encapsulation platforms.[30] By matching the size of the enzyme with that of the large channel, various enzymes could be encapsulated.

We reasoned that the large mesoporous channels of the zirconium MOF PCN-128y (4.4 nm)[31] should be ideal for confining but not constricting the wild-type OPAA (from bacterium *Alteromonas sp.* JD6.5, 440 amino acid),[32] a protein featuring a small-axis length of ∼4.4 nm, in highly concentrated, yet nonaggregated, form (Figure 1a). In contrast, the narrower triangular channels (micropores) of PCN-128y should effectively exclude OPAA, leaving them free instead to transport molecule-sized reactants and products. Windows between small and large channels, present in high density,

Received: April 9, 2016
Published: June 24, 2016

DOI: 10.1021/jacs.6b03673
J. Am. Chem. Soc. 2016, 138, 8052−8055

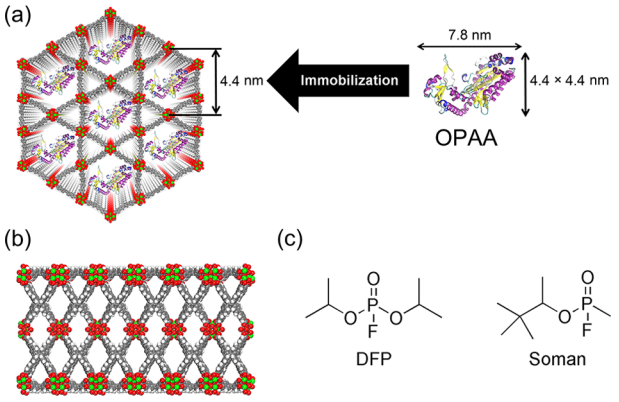

Figure 1. (a) Immobilization of OPAA in the mesoporous channels of PCN-128y. (b) Side view of PCN-128y with open windows between mesoporous channels and microporous channels (Zr atoms are shown in green, C atoms in gray, O atoms in red, and H atoms in white). (c) Chemical structures of nerve agents used in this study.

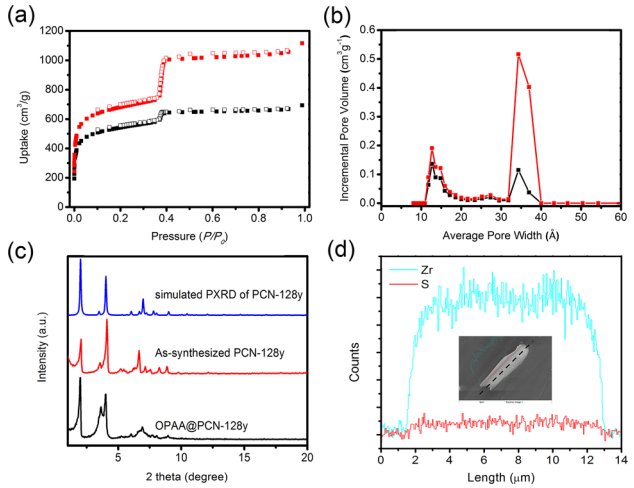

Figure 2. (a) N_2 adsorption−desorption isotherms. (b) DFT pore size distributions for PCN-128y (red) and OPAA@PCN-128y (black). (c) PXRD patterns of simulated PCN-128y, experimental PCN-128y, and OPAA@PCN-128y. (d) SEM image and EDX spectra of a single crystal of OPAA@ CN-128y. EDX scan lines for Zr and S are, respectively, in cyan and red. The dashed black line indicates where the EDX scan was taken.

should permit reactants to readily access the immobilized OPAA (Figure 1b). These features, combined with the high chemical and thermal stability of PCN-128y,[31] make this MOF a promising candidate material for the preparation of an immobilized nerve agent antidote. Herein we report the successful encapsulation and characterization of OPAA in PCN-128y and its catalytic performance in detoxifying the nerve agent simulant diisopropyl fluorophosphate (DFP) and the real nerve agent *O*-pinacolyl methyl fluorophosphonate (Soman) (Figure 1c). More importantly, the immobilized OPAA shows higher thermal stability than the free enzyme and superior long-term storage stability.

To immobilize OPAA, we treated activated crystals of PCN-128y with a bis-tris-propane buffer (BTP) solution of OPAA (0.2 mg/mL, pH 7.2) at 25 °C (Figure 1). The uptake of OPAA by PCN-128y was followed using UV−vis spectroscopy, and a maximum loading of 0.10−0.12 mg/mg was reached after 24 h (Figure S1). The solid sample (hereafter denoted as OPAA@PCN-128y) was then washed with BTP buffer solution five times to remove the OPAA adsorbed on the surface. To confirm the loading of OPAA in PCN-128y, inductively coupled plasma−optical emission spectroscopy (ICP-OES) was used to measure the ratio of Zr (Zr nodes in MOF) to S (methionines and cysteines in OPAA) in the digested OPAA@ PCN-128y samples. The ICP analysis confirms an OPAA uptake of 0.12 mg/mg. To the our knowledge, the OPAA loading capacity of PCN-128y is much higher than that of any other porous material yet examined.[15,33] The N_2 adsorption isotherm of OPAA@PCN-b128y exhibits a lower N_2 uptake capacity than that of PCN-128y (Figure 2a). The density functional theory (DFT) pore size distribution analysis of PCN-128y and OPAA@PCN-128y shows that the pore volume corresponding to the triangular channels (1.2−1.5 nm) of PCN-128y drops from 0.19 to 0.14 cm^3/g, while the incremental pore volume corresponding to the hexagonal channels (3.3−4.0 nm) drops from 0.52 to 0.13 cm^3/g after OPAA encapsulation (Figure 2b). These results are in agreement with the contention that a considerable portion of the mesopores in PCN-128y are occupied by OPAA, while the micropores in PCN-128y are still mostly empty. The powder X-ray diffraction (PXRD) patterns and scanning electron microscopy (SEM) images of PCN-128y before and after OPAA immobilization confirm that bulk crystallinity and morphology of PCN-128y are retained (Figures 2c and S2). To determine the distribution of OPAA in PCN-128y crystals, we used *in situ* confocal laser scanning microscopy (CLSM) to image AlexaFluor-647-tagged OPAA in crystals of PCN-128y at different depths (Figure S3).[34] Comparison of CLSM micrographs from the bottom to the top of a 5 μm *z*-axis height indicates that OPAA is not only on the surface of PCN-128y but also is dispersed throughout the PCN-128y crystals. In addition, SEM-EDX images show an even distribution of sulfur along a single crystal of PCN-128y, which further confirms that OPAA is dispersed throughout the MOF (Figure 2d).

We next examined the enzyme activity and encapsulation efficacy of OPAA@PCN-128y by utilizing a less toxic nerve agent simulant diisopropyl fluorophosphate (DFP) as a model substrate (Figure S4). Previous studies have demonstrated that zirconium MOFs themselves[35,36] are excellent nerve agent detoxification catalysts, but only in buffered solutions at pH values of ~8.5 and higher.[37] Enzyme-free PCN-128y in pH 7.2 BTP buffer, however, shows no catalytic activity, and the hydrolysis of DFP is not evident (Figure 3a). Compared to free OPAA under the same conditions, the initial rate of DFP hydolysis rate of OPAA@PCN-128y is comparatively low possibly due to slow intra-MOF diffusion by reactants and products (Figure 3a).[38] Nevertheless, for both free OPAA and OPAA@PCN-128y as catalysts, the conversion of DFP plateaus at 80−90%. To examine the enzyme accessibility after immobilization, composites with different enzyme loadings were prepared and tested for DFP hydrolysis (Figure S5). The results indicate that the activity of composites systematically increased as the enzyme loadings. To assess enzyme thermal stability, we measured the extent of hydrolytic degradation of DFP achieved over a range of incubation/reaction temperatures using free versus encapsulated OPAA as the catalyst (Figures 3b and S6). Both free OPAA and OPAA@PCN-128y show optimal activity after incubation at 45 °C. However, the incubation of free OPAA at 55 °C results in a significant loss of the conversion of DFP, indicating the loss of enzymatic activity. In contrast, OPAA@PCN-128y yielded around 90% con-

DOI: 10.1021/jacs.6b03673
J. Am. Chem. Soc. 2016, 138, 8052−8055

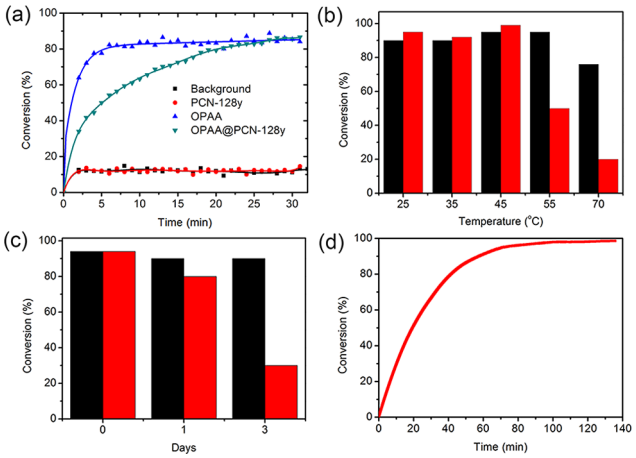

Figure 3. (a) Reaction profile of DFP hydrolysis by free OPAA (blue), OPAA@PCN-128y (green), PCN-128y (red), and the background reaction (black). (b) Thermal stability as measured in terms of conversion of DFP hydrolysis upon incubating at increasing temperatures (black bar for OPAA@PCN-128y and red bar for free OPAA) (c) Long-term stability as measured in terms of conversion of DFP hydrolysis after room temperature storage in dry powder form over time (black bar for OPAA@PCN-128y and red bar for free OPAA). (d) Reaction profile of Soman hydrolysis by OPAA@PCN-128y.

version. When we further increased the incubation temperature to 70 °C, the OPAA@PCN-128y showed remarkable stability and a conversion of almost 75%. In contrast, the low conversion for free OPAA at 70 °C suggests that free OPAA is denatured at this temperature.

Encouraged by the high thermal stability of OPAA encapsulated in PCN-128y, we sought to address the issue of long-term stability, an important one for field applications issue of OPAA or other detoxification enzymes. To assess temporal stability, the as-synthesized OPAA@PCN-128y was air-dried, and free OPAA was lyophilized. Both dried samples were then stored at room temperature, with smaller samples being removed and tested after storage for various lengths of time (Figures 3c and S7). Stability was measured by determining the conversion of DFP using the same conditions used previously. Initially, when reintroduced to DFP solutions, both the dried OPAA@PCN-128y and lyophilized OPAA achieve nearly 90% conversion. For lyophilized OPAA subjected to 1 day of dry storage, conversion plateaued at 79%, implying some loss of stability. After 3 days of dry, lyophilized free OPAA proved capable of catalyzing hydrolysis of 30% of the DFP present. In striking contrast, even after 3 days of dry storage, OPAA@PCN-128y remained capable of catalyzing the hydrolysis of 90% of the DFP present. These results show that the MOF can be used to protect and stabilize OPAA, which is important for a portable antidote material to be used in extreme conditions (such as high temperatures in the desert with low humidity). To further demonstrate the efficacy of OPAA@PCN-128y as a decontaminant for G-type nerve agents, we examined its catalytic performance for the hydrolysis of the real nerve agent, Soman. *Caution: Soman is deadly. It can be safely and legally studied only by specifically trained and authorized personnel working in secure, approved facilities.* The results indicate that OPAA@PCN-128y can efficiently defluorinate/deactivate Soman (thereby removing the leaving group that enables its binding to acetylcholinesterase). By using an F^- electrode, the initial reaction rate was calculated to be in the range of 56−75 μmol/min/mg (Figure S8). Similar to its behavior in the hydrolysis of DFP, OPAA@PCN-128y hydrolyzes Soman and reaches 90% conversion in 60 min using 3.75 μg OPAA@PCN-128y on 3 mM Soman at 25 °C (Figure 3d).

In summary, the water-stable mesoporous channel-type zirconium MOF PCN-128y is shown to be capable of encapsulating OPAA with a high loading. This size-matching encapsulation process is performed rapidly under mild conditions and requires no prior chemical modification of the protein of interest. More importantly, following OPAA uptake by the large (mesoporous) channels of PCN-128y, the smaller channels (microporoes) of the hierarchically structured host material remain open and available as conduits for reactant and product diffusion to and from the active sites of the encapsulated enzymes. In addition, we have shown that PCN-128y excels at stabilizing the enzyme at high temperature and in dry-form, whereas the free enzyme degrades rapidly under these conditions. These findings suggest that MOF encapsulated OPAA (or related enzymes) may be suitable for large area and personnel decontamination.

■ ASSOCIATED CONTENT

Supporting Information

The Supporting Information is available free of charge on the ACS Publications website at DOI: 10.1021/jacs.6b03673.

CLSM, kinetic reaction plots of DFP and Soman hydrolysis, and additional figures (PDF)

■ AUTHOR INFORMATION

Corresponding Author

*o-farha@northwestern.edu

Notes

The authors declare no competing financial interest.

■ ACKNOWLEDGMENTS

O.K.F. and J.T.H. gratefully acknowledge DTRA for financial support (HDTRA1-14-1-0014). The authors thank Dr. Brian Pate (Joint Science & Technology Office for Chemical & Biological Defense, Defense Threat Reduction Agency) for helpful discussions. S.P.H. and M.A.G. gratefully acknowledge DTRA for financial support.

■ REFERENCES

(1) Bajgar, J. *Adv. Clin. Chem.* **2004**, *38*, 151−216.
(2) Yang, Y.-C. *Acc. Chem. Res.* **1999**, *32*, 109−115.
(3) Firozjaei, S. A. A.; Latifi, A. M.; Khodi, S.; Abolmaali, S.; Choopani, A. *J. Appl. Biotechnol. Rep.* **2015**, *2*, 215−224.
(4) Newmark, J. *Arch. Neurol.* **2004**, *61*, 649−652.
(5) Ghanem, E.; Raushel, F. M. *Toxicol. Appl. Pharmacol.* **2005**, *207*, 459−470.
(6) Nachon, F.; Brazzolotto, X.; Trovaslet, M.; Masson, P. *Chem.-Biol. Interact.* **2013**, *206*, 536−544.
(7) Tsai, P.-C.; Fox, N.; Bigley, A. N.; Harvey, S. P.; Barondeau, D. P.; Raushel, F. M. *Biochemistry* **2012**, *51*, 6463−6475.
(8) Raushel, F. M. *Nature* **2011**, *469*, 310−311.
(9) Daczkowski, C. M.; Pegan, S. D.; Harvey, S. P. *Biochemistry* **2015**, *54*, 6423−6433.
(10) Hoskin, F.; Roush, A. H. *Science* **1982**, *215*, 1255−1257.
(11) Cheng, T.-C.; DeFrank, J. J.; Harvey, S. P.; Rastogi, V. K. U.S. Patent 7229819, June 12, 2007.
(12) Yin, R.; Cheng, T. C.; Durst, H. D.; Qin, D. U.S. Patent 6716450, May 17, 2004.

DOI: 10.1021/jacs.6b03673
J. Am. Chem. Soc. 2016, 138, 8052−8055

(13) Simonian, A.; Grimsley, J.; Flounders, A.; Schoeniger, J.; Cheng, T.-C.; DeFrank, J.; Wild, J. *Anal. Chim. Acta* **2001**, *442*, 15−23.
(14) Chen, B.; Shah, S. S.; Shin, Y.; Lei, C.; Liu, J. *Anal. Biochem.* **2012**, *421*, 477−481.
(15) Ong, K. K. Encapsulation of organophosphorus acid anhydrolase (OPAA) in nanostructured materials for the detection and decontamination of chemical warfare agents. *Ph.D. Thesis*, Drexel University, May, 2006.
(16) Létant, S. E.; Kane, S. R.; Hart, B. R.; Hadi, M. Z.; Cheng, T.-C.; Rastogi, V. K.; Reynolds, J. G. *Chem. Commun.* **2005**, *7*, 851−853.
(17) Furukawa, H.; Cordova, K. E.; O'Keeffe, M.; Yaghi, O. M. *Science* **2013**, *341*, 1230444.
(18) Fried, D. I.; Brieler, F. J.; Fröba, M. *ChemCatChem* **2013**, *5*, 862−884.
(19) Lykourinou, V.; Chen, Y.; Wang, X.-S.; Meng, L.; Hoang, T.; Ming, L.-J.; Musselman, R. L.; Ma, S. *J. Am. Chem. Soc.* **2011**, *133*, 10382−10385.
(20) Chen, Y.; Lykourinou, V.; Hoang, T.; Ming, L.-J.; Ma, S. *Inorg. Chem.* **2012**, *51*, 9156−9158.
(21) Feng, D.; Liu, T.-F.; Su, J.; Bosch, M.; Wei, Z.; Wan, W.; Yuan, D.; Chen, Y.-P.; Wang, X.; Wang, K.; Lian, X.; Gu, Z.-Y.; Park, J.; Zou, X.; Zhou, H.-C. *Nat. Commun.* **2015**, *6*, 5979.
(22) Ockwig, N. W.; Delgado-Friedrichs, O.; O'Keeffe, M.; Yaghi, O. M. *Acc. Chem. Res.* **2005**, *38*, 176−182.
(23) Deng, H.; Grunder, S.; Cordova, K. E.; Valente, C.; Furukawa, H.; Hmadeh, M.; Gándara, F.; Whalley, A. C.; Liu, Z.; Asahina, S.; Kazumori, H.; O'Keeffe, M.; Terasaki, O.; Stoddart, J. F.; Yaghi, O. M. *Science* **2012**, *336*, 1018−1023.
(24) Furukawa, H.; Gándara, F.; Zhang, Y.-B.; Jiang, J.; Queen, W. L.; Hudson, M. R.; Yaghi, O. M. *J. Am. Chem. Soc.* **2014**, *136*, 4369−4381.
(25) Burtch, N. C.; Jasuja, H.; Walton, K. S. *Chem. Rev.* **2014**, *114*, 10575−10612.
(26) Mondloch, J. E.; Bury, W.; Fairen-Jimenez, D.; Kwon, S.; DeMarco, E. J.; Weston, M. H.; Sarjeant, A. A.; Nguyen, S. T.; Stair, P. C.; Snurr, R. Q.; Farha, O. K.; Hupp, J. T. *J. Am. Chem. Soc.* **2013**, *135*, 10294−10297.
(27) Feng, D.; Gu, Z.-Y.; Li, J.-R.; Jiang, H.-L.; Wei, Z.; Zhou, H.-C. *Angew. Chem., Int. Ed.* **2012**, *51*, 10307−10310.
(28) Morris, W.; Volosskiy, B.; Demir, S.; Gándara, F.; McGrier, P. L.; Furukawa, H.; Cascio, D.; Stoddart, J. F.; Yaghi, O. M. *Inorg. Chem.* **2012**, *51*, 6443−6445.
(29) Gomez-Gualdron, D. A.; Gutov, O. V.; Krungleviciute, V.; Borah, B.; Mondloch, J. E.; Hupp, J. T.; Yildirim, T.; Farha, O. K.; Snurr, R. Q. *Chem. Mater.* **2014**, *26*, 5632−5639.
(30) Li, P.; Modica, J. A.; Howarth, A. J.; Vargas, E.; Moghadam, P. Z.; Snurr, R. Q.; Mrksich, M.; Hupp, J. T.; Farha, O. K. *Chem.* DOI: 10.1016/j.chempr.2016.05.001.
(31) Zhang, Q.; Su, J.; Feng, D.; Wei, Z.; Zou, X.; Zhou, H.-C. *J. Am. Chem. Soc.* **2015**, *137*, 10064−10067.
(32) Cheng, T.; Harvey, S. P.; Chen, G. L. *Appl. Environ. Microbiol.* **1996**, *62*, 1636−1641.
(33) El-Boubbou, K.; Schofield, D. A.; Landry, C. C. *J. Phys. Chem. C* **2012**, *116*, 17501−17506.
(34) Zavattini, G.; Vecchi, S.; Mitchell, G.; Weisser, U.; Leahy, R. M.; Pichler, B. J.; Smith, D. J.; Cherry, S. R. *Phys. Med. Biol.* **2006**, *51*, 2029.
(35) Mondloch, J. E.; Katz, M. J.; Isley Iii, W. C.; Ghosh, P.; Liao, P.; Bury, W.; Wagner, G. W.; Hall, M. G.; DeCoste, J. B.; Peterson, G. W.; Snurr, R. Q.; Cramer, C. J.; Hupp, J. T.; Farha, O. K. *Nat. Mater.* **2015**, *14*, 512−516.
(36) Li, P.; Klet, R. C.; Moon, S.-Y.; Wang, T. C.; Deria, P.; Peters, A. W.; Klahr, B. M.; Park, H.-J.; Al-Juaid, S. S.; Hupp, J. T.; Farha, O. K. *Chem. Commun.* **2015**, *51*, 10925−10928.
(37) An exception is the zirconium-MOF-catalyzed degradation of the nerve agent VX, which can be accomplished at pH 7.
(38) Consistent with this idea, we have observed (with an enzyme-free MOF catalyst) that rates of reactions can be substantially enhanced by reducing MOF crystallite sizes and thereby decreasing intra-MOF diffusion distances for molecular reactants; see ref 36.

DOI: 10.1021/jacs.6b03673
J. Am. Chem. Soc. 2016, 138, 8052−8055